Electronic structure, magnetic, and electrical properties of single-crystalline magnetic fluctuator URuAl and comparison with reference systems

M. Samsel-Czekała,[1,2] E. Talik,[3] and R. Troć[2]

[1]*Leibniz-Institut für Festkörper-und Werkstoffforschung, IFW Dresden, PF 270116, D-01171 Dresden, Germany*

[2]*Institute of Low Temperature and Structure Research, Polish Academy of Sciences, P.O. Box 1410, 50-950 Wrocław 2, Poland*

[3]*Institute of Physics, University of Silesia, Uniwersytecka 4, 40-007 Katowice, Poland*

(Received 8 July 2008; revised manuscript received 3 November 2008; published 24 December 2008)

The electronic structure of the hexagonal paramagnetic ternary intermetallic compound URuAl is computed, employing the full relativistic version of full-potential local-orbital band-structure code, and examined by x-ray photoelectron spectroscopy (XPS) of both valence bands and 4*f* core levels. Satisfying agreement between experimental and theoretical XPS results is achieved indicating high delocalization of the U 5*f* states in this intermetallic compound. The Fermi surface of URuAl has been calculated and discussed as well. The previously reported possibility of an existence of spin (magnetic) fluctuations in URuAl has also been supported by our data based on, e.g., 4*f*-core XPS spectra, magnetization, magnetic susceptibility, electrical resistivity, and magnetoresistivity ones. The lack of magnetic ordering in URuAl is discussed in comparison to other similar systems U*T*(Al,Ga) and their solid solutions, where *T* is a transition metal.

DOI: 10.1103/PhysRevB.78.245120 PACS number(s): 71.20.−b, 79.60.−i, 72.15.Eb, 75.47.−m

I. INTRODUCTION

URuAl crystallizes in a very common crystal structure of the hexagonal ZrNiAl-type (space group: *P*-62*m*) as does also URuGa and both are paramagnetic (PM) down to 20 mK.[1] This layered type of structure is popular in a large series of the U*TM* ternaries (*T* is a 3*d*, 4*d*, and 5*d* transition metal and *M*=Al, Ga, Sn, In, Sb). It consists of two types of basal-plane layers, containing U,*T*(1) and *M*,*T*(2) atoms alternating along the crystallographic *c* axis. In this structure, uranium atoms form a distorted Kagomé lattice within their basal plane. As a consequence the coordination of magnetic uranium moments may lead to a geometrical frustration in the case of their antiferromagnetic (AFM) arrangement. In such a situation, this makes a problem of magnetic ordering in ZrNiAl-type lattice causing very complex magnetic structures as, e.g., for UNiAl.[2] The propagation vector of this structure is unusual and amounts $\mathbf{q}=[0.1,0.1,0.5]$. The magnetic moments are ordered along the *c* axis being sine-wave modulated but within the basal plane with a period of 10 a_0. Therefore, this is not surprising that most of UTM compounds with the above crystal structure choose a ferromagnetic (FM) order. In contrast, UCoAl, URuAl, and URuGa remain PM to the lowest temperatures though this paramagnetism is temperature dependent and exhibits huge anisotropy. Quite a different behavior is that of UFeAl. This ternary aluminide is classified as an isotropic Pauli paramagnet (PP). In URuAl the U-U nearest distance of 0.36 nm (for the U atoms within the basal plane) is close to so-called Hill limit of 0.35 nm, so that one strongly expects that this should lead to a partial delocalization of the 5*f* states probably due to a transfer of some 5*f* electrons into the U 6*d* and other ligand states. Such a behavior results first of all from a strong 5*f*-6*d* hybridization and, as a consequence, a broadening of the 5*f* level into a narrow density of states (DOS) takes place (the bandwidth *W* is of the order of eV) with its maximum close to the Fermi level (E_F) and, in addition, to spreading these states into a wide band with a small intensity of DOS across several eV, as it was described schematically in Ref. 3. Hence, for such materials as the equivalent 1:1:1 uranium intermetallics one has to do with a variety of physical behaviors but especially with a variation of magnetic properties from enhanced PPs to magnetic (spin) fluctuation systems and, finally, to a local-moment behavior, depending on the position of given *T* and *M* atoms in the periodic table.

In the past, temperature dependence of the susceptibility of URuAl on the polycrystalline sample was studied by several authors.[1,4,5] On this basis this compound was considered as a spin-fluctuation system.[1] Then, single-crystalline studies[6] have allowed to observe the huge uniaxial magnetocrystalline anisotropy in the PM state, caused not only by a crystal-field interaction but mainly by a dominating hybridization-induced effect.[7] The susceptibility for an applied field along the *c* axis, $\chi_c(T)$, is much larger than that in a perpendicular field, $\chi_a(T)$. The low-temperature susceptibility deviates considerably from a regular temperature variation being characterized by the broad maximum around 50 K for both main crystallographic directions, much pronounced especially in the case of $\chi_c(T)$. Above 100 K both susceptibility curves measured along the *c* and *a* axes can be fitted by a modified Curie-Weiss (CW) law with the following parameters: $\Theta_p=-53$ K and $\mu_{\text{eff}}=2.24$ μ_B and with $\Theta_p=-410$ K and $\mu_{\text{eff}}=2.3$ μ_B, respectively. For these directions the same value of χ_0 $(0.64\times10^{-3}$ emu/mol) has been derived.[6] So single-crystalline materials of the uniaxial lattice symmetry as hexagonal one give the possibility of an unambiguous interpretation of bulk magnetic results and a presentation of their huge anisotropy. The anisotropy in a simple way can be expressed by the difference $\Delta\Theta_p=(\Theta_p^c-\Theta_p^{ab})$. Taking into account the above paramagnetic Curie temperatures, it yields 357 K.[8]

In URuAl, except for anomalous temperature dependences of the susceptibility, also an anomaly in magnetization in high magnetic fields up to 35 T (Refs. 8 and 9) and 60 T (Ref. 10) has been observed. Namely, the magnetization curve at 4.2 K in fields applied along the *c* axis exhibits a

small upturn above 20 T followed by a gradual tendency to saturation above 35 T. The high-field susceptibility has a maximum around 30 T. The characteristics energy of this anomaly can be related to the characteristics energy of the $\chi_c(T)$ maximum at 50 K.

In turn, magnetization density studies of URuAl made by Paixão *et al.*[11] using polarized-neutron experiment on a single crystal have allowed the observation of an essential magnetization density induced at the U and Ru sites in the U-Ru basal plane owing to the hybridization between the U $5f$ and Ru $4d$ states. These results have clearly proved the existence of the large anisotropic $5f$-ligand hybridization effects. It was suggested[7,11] that a mechanism of this large anisotropy may arise from the anisotropic chemical bonding of $5f$ electrons in the ZrNiAl lattice leading to anisotropic exchange intersections between the $5f$ magnetic moments.[8,10] However, as shown in Ref. 11 the hybridization is independent of the exchange interactions and the latter cannot be solely responsible for the anisotropy. Therefore, the origin of the anisotropy remains still unclear.

Some interesting properties of URuAl have been derived from studies of a number of solid solutions, e.g., of the $U(T_{1-x}Ru_x)Al$ or $URu(M_{1-x}Al_x)$ types. For example, FM was observed in a wide concentration range of solid solutions such as $UCo_{1-x}Ru_xAl$,[12–14] in which already 1% substitution of Ru for Co is enough to bring about this ordered state at low temperature, though as already mentioned above the parent compounds, UCoAl and URuAl, have a nonmagnetic ground state.[1] Both the spontaneous moment and ordering temperature grow rapidly with increasing x, reaching their maximum values around $x=0.3$, and then they monotonically decrease with further increasing Ru content up to $x=0.8$, where FM completely disappears. Interestingly, very similar properties are also exhibited by the $U(Ru_{1-x}Rh_x)Al$ systems,[4,5,10] but this time URhAl is already a ferromagnet with $T_C=35$ K.

For another pseudoternary system $U(Ni_{1-x}Ru_x)Al$ a more complex evolution of magnetism has been observed[15] mainly due to the AFM properties of the parent compound UNiAl. In this system AFM is rapidly suppressed and already for $x=0.15$ the FM state occurs which exists in a wide concentration region $0.15 \leq x \leq 0.95$, exhibiting the concentration dependencies of the ordering temperature and spontaneous moment which form a pronounced maxima for intermediate concentrations, as in the systems mentioned above. In a similar way, the AFM region of stability can be dramatically reduced by substitution of Fe for Ni in the solid solutions: $U(Fe_{1-x}Ni_x)Al$,[16,17] despite the fact of PP in UFeAl. It is interesting to note that even in the case of nonmagnetic properties of the latter compound, FM was revealed in a wide concentration range $0.2 \leq x \leq 0.65$, with going through maxima in T_C and spontaneous moment for $x=0.5$, in a similar way as for the system based on Ru.

Finally, it should be mentioned also the quasiternary system $URu(Al_{1-x}Sn_x)$, where the boundary end compound, namely, URuSn, is a ferromagnet like URhAl, but with higher T_C(=55 K). The onset of FM, as in other systems considered here, already occurs at $x=0.2$ but this time with a monotonous increase of both magnetic moment and T_C with increasing Sn content.[18]

Up to now, only studies of electrical resistivity on polycrystalline sample of URuAl have been performed and presented in a normalized form.[19] The observed temperature dependence of the resistivity was very weak at high values of temperature and revealed a pronounced knee around 50 K. The above aspects of the behavior will be discussed later on.

Up to our best knowledge, for URuAl there has been only scalar-relativistic linear muffin-tin orbital (LMTO)-atomic sphere approximation (ASA) band-structure calculations reported,[20–22] but no x-ray photoelectron spectroscopy (XPS) measurements have been performed so far for U*TM* compounds, except for URuGa,[23] with the ZrNiAl structure. In contrast to previous band-structure treatment of URuAl, the present paper reports results of full potential and full relativistic band-structure calculations within the full-potential local-orbital (FPLO) minimum basis code.[24] They are compared with our experimental XPS data obtained on a single crystal of URuAl as well as the differences between our and previously published calculations for this aluminide are discussed. We present here also results of bulk measurements as magnetization, susceptibility, electrical resistivity, and magnetoresistivity performed on single-crystalline samples.

II. EXPERIMENT

A single crystal of URuAl has been prepared from a stoichiometric melted constituents by the Czochralski method with starting elements (of purity in weight percent) U (99.98), Ru (99.99), and Al (99.999). No further heat treatment was performed to the as-grown single-crystal button. Electron microprobe analyzes were used to verify the good quality of the obtained single crystals. The button was cut by an abrasive tungsten wire into pieces with appropriate geometries suited to different kind measurements.

The XPS spectrum was recorded at room temperature (RT) in a PHI 5700/660 physical electronic photoelectron spectrometer using a monochromatized Al K_α x-ray source ($h\nu=1486.6$ eV).[25] The angle between the x-ray beam and the sample surface was 45°. All measurements were performed under ultrahigh vacuum (UHV) condition in the range 10^{-10} Torr on the URuAl surface, obtained by cleaving the (100) planes *in situ* and immediately after that the measurements were carried out. The energy spectra of the electrons were analyzed by a hemispherical mirror analyzer with an energy resolution of 0.3 eV. The Fermi level was referred to the gold $4f$ at 84 eV of binding energy (BE). The single-crystalline sample of URuAl, after breaking in UHV condition, produced an overall spectrum with only negligible oxygen contamination. In the whole region of the measured spectrum (−1400−1 eV) there are only small traces of the O($1s$) and O (KLL) at the −532 and −975 eV BE, respectively, and the distinct lack of the peak O($2s$) near −6 eV. The investigated sample did not show signs of any surface degradation during the XPS experiment.

Magnetization and magnetic-susceptibility measurements were carried out using a commercial superconducting quantum interference device (SQUID) magnetometer in the temperature region from 1.9 up to 400 K and in fields up to 5 T with the sample oriented along the main crystallographic

axes using the x-ray method. The electronic transport was measured employing a steady-current four-point method with spot-welded wire contacts on bar-shaped specimens of $1 \times 1 \times 5$ mm^3 dimension at temperatures between 4.2 and 290 K and in transverse magnetic fields ($\mathbf{j} \perp \mathbf{B}$) up to $B = \mu_0 H = 8$ T.

III. THEORY

The band structure of URuAl has been computed by the fully relativistic version of the FPLO method.[24] In this approach the four-component Kohn-Sham-Dirac equation, containing implicitly spin-orbit coupling (SOC) up to all orders, is solved self-consistently. The Perdew-Wang parametrization[26] of the exchange-correlation potential in the local (spin)-density approximation [L(S)DA] with and without an orbital polarization correction (OPC) (Ref. 27) was utilized. For the calculations experimental values of both lattice parameters $a=0.6866$ nm, $c=0.4026$ nm, and the following atomic positions in the unit cell: for U: (0.57993, 0, 0.5); Ru(1): (0,0, 0.5); Ru(2): (1/3, 2/3, 0); Al: (0.23646, 0, 0), determined at 120 K, were taken from Ref. 28. The valence basis sets were used as follows: the U $5d5f;6s6p6d;7s7p$, the Ru(1) and Ru(2) $4s4p4d;5s5p$, and the Al $2s2p;3s3p3d$ states. The higher-lying $5d;6s6p$ semicore uranium states that have a possibility of hybridizing with the $6d$ and $5f$ valence states were also included in the basis. The maximum size of the k-point mesh in the Brillouin zone (BZ) was $20 \times 20 \times 20$, though the mesh $12 \times 12 \times 12$ turned out to be sufficient.

The band energies, $E_n(\mathbf{k})$, Fermi surface (FS), as well as total and partial DOS per formula unit (f.u.) were calculated within local-density approximation (LDA). The latter were computed for each atomic site in the unit cell ($Z=3$ f.u.) and for all atomic states considered separately. For comparison with the experimental XPS, the theoretical valence-band XPS spectrum was calculated by the standard procedure, neglecting an evaluation of energy-dependent transition matrix elements as done, e.g., in Ref. 29. Namely, the partial DOSs for the constituent atoms were multiplied by the respective weight factors proportional to atomic subshell photoionization cross sections.[30] The outputs were summed up and convoluted with a Gaussian of full width at the half maximum being equal to 0.3 eV to simulate the instrumental energy resolution of the experimental analyzer.

Additionally, spin- and orbital-polarized calculations within LSDA and LSDA+OPC were performed to find the total energy of a possible ferromagnetic arrangement along the hexagonal c axis and values of ordered magnetic moments.

IV. RESULTS

A. Electronic structure calculations and x-ray photoelectron spectroscopy

The determined, based on LDA, band energies, $E_n(\mathbf{k})$, in URuAl are displayed in the vicinity of E_F in Fig. 1. They exhibit metallic-type behavior as expected from experiments. The bands crossing E_F are dominated by the U $5f_{5/2}$ states being strongly hybridized with the U $6d$ and Ru(1) and Ru(2) $4d$ as well as the Al $3sp$ states. It is well visible in Fig. 2 where we have plotted the corresponding total and partial DOSs.

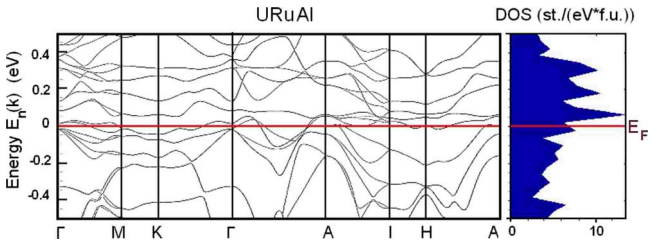

FIG. 1. (Color online) Computed energy bands $E_n(\mathbf{k})$ and total DOS in URuAl around E_F.

From these calculations a very broad and complex contribution from the U $5f$ states appears, ranging from 4.2 eV below E_F and even up to 6 eV above E_F. In addition, a small trace of these states occurs in the range of 5–6 eV below E_F. As usually in UTM compounds, the SOC leads to two main U $5f$ peaks, split into the states $5f_{5/2}$ and $5f_{7/2}$ (in energy range between −1 and 2.5 eV), shifted from each other by about 1 eV. The lower energy peak of the U $5f_{5/2}$ states cuts the Fermi level yielding a relatively high DOS at E_F, although the calculated value of the electronic specific-heat coefficient $\gamma_b = 3.0$ mJK^{-2} mol^{-1} is 15 times smaller than the

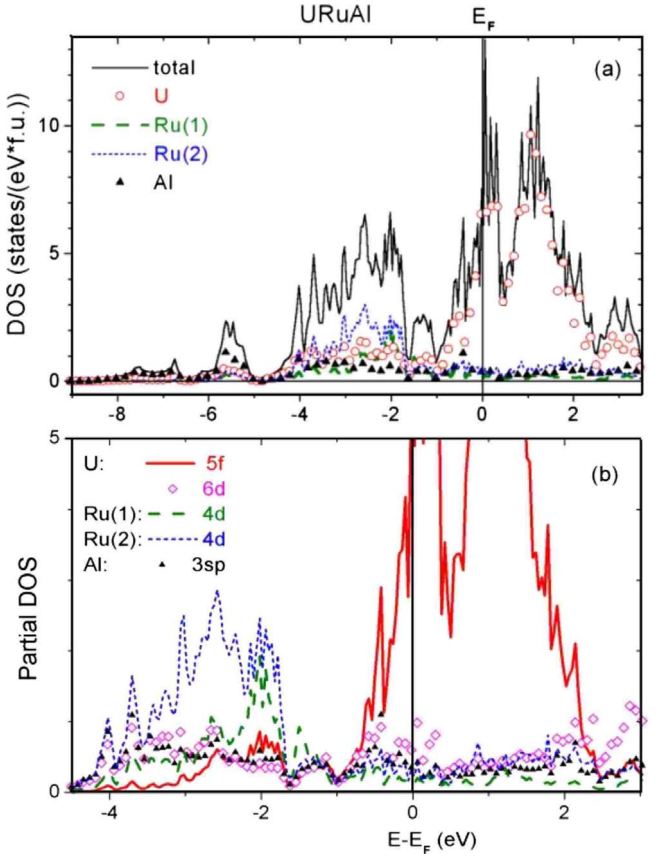

FIG. 2. (Color online) Computed DOSs in URuAl: total and partial (on atomic sites) (a) as well as for different electron states (b).

experimental value $\gamma(0)=45$ mJK^{-2} mol^{-1}.[1] Another pronounced but broad contribution originating from the U 5*f* electrons occurs between 1 and 4.2 eV below E_F (see Fig. 2).

There is also a wide (flat) contribution from the U 6*d* states in the same energy range as the U 5*f* states, hybridizing with the latter, which leads to metallic bonding between U-U atoms in URuAl. It is visible from Fig. 2(b) that the contributions at E_F from the Ru(1) and Ru(2) 4*d* states as well as from the Al 3*sp* states seem to be to some extent pronounced and comparable to one another. In the energy range from 1 to 5 eV below E_F, there are much higher and different from each other contributions of the ruthenium 4*d* states originating from different atomic sites, Ru(1) and Ru(2). These states also hybridize with the U 5*f*6*d* states and Al 3*spd* ones. Moreover, in the energy range of 5–6 eV below E_F, there is a fairly large contribution of the Al 3*sp* states hybridizing with relatively high contributions coming from the U 6*d* states (including small traces of the 5*f* states) and the ruthenium 4*d* states.

Based on the electron population analysis, the occupation number, *N*, of the U 5*f* states is reduced from 3 to 2.75, for the U 6*d* states *N* is enhanced from 1 to 2.36 electrons per atom, while for the U 7*s* states it is much reduced from 2 to 0.54 electrons compared to those of free-atom occupations. Furthermore, the numbers of 5*s* states coming from Ru(1) and Ru(2) atoms are also reduced from $N=1$ to 0.38 and 0.49, respectively. In turn, the ruthenium 5*p* states occur with *N* equal to 0.31 and 0.45. It is worth underlining that for the Ru 4*d* states N is only slightly increased from a nominal atomic value of 7 to 7.01 and 7.05 for Ru(1) and Ru(2), respectively. In the case of aluminum, the 3*s* states again strongly reduced their N from 2 to 1.10 whereas the 3*p* states essentially increased their N from 1 to 1.63 electrons as well as the 3*d* states occur with high N of 0.47 electrons per one atom. Summarizing, there is quite a large charge transfer of 0.52 valence electrons from U atoms and a small transfer of 0.09 from Ru(1) (within the U plane) to aluminum (0.49) and to Ru(2) (0.12) per f.u. It is worth noticing that the electron transfers occurring for different atomic positions, Ru(1) and Ru(2), are opposite to each other.

The calculated Fermi surface of URuAl, presented in Fig. 3, exists in four bands (151–154). Since this is a compensated metal, the total volume of occupied states (electrons) should be the same as that of unoccupied states (holes). The FS sheets in the first two conduction bands contain only very small hole pockets around the *A* points (excluding the very vicinity of *A* points) and, additionally, close to the Γ point, but the latter only in the second band. There are three types of disconnected hole FS sheets in the third band: a big distorted ball around the Γ point, rosette centered at the *A* point, and monster arms fixed at the *L* points. FS in the fourth conduction band consists of three types of closed and opened electron pieces with the dominating crone in the middle of BZ. It is worth noticing that all FS elements are disconnected along the hexagonal axis and in this direction the central elements in the second, third, and fourth bands have geometry typical of nesting (flat parallel parts of FS sheets) that may mediate in magnetic interactions, connected with magnetic fluctuations. Experimentally, such a nesting (or webbing) of FS was observed by measuring angular correlation

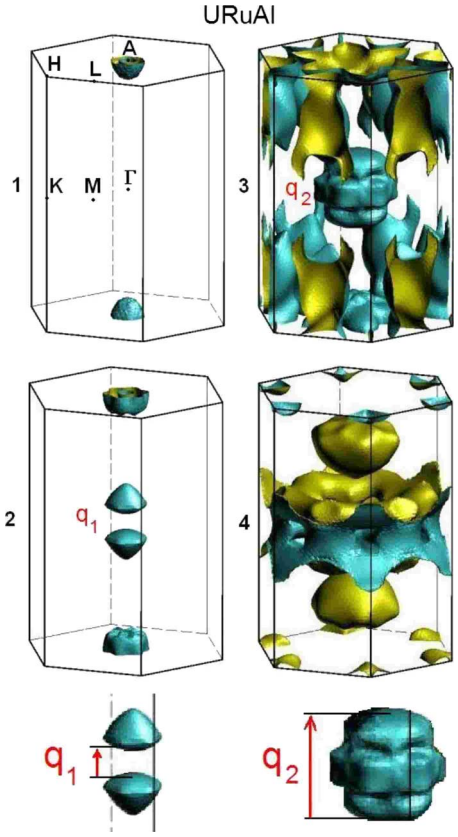

FIG. 3. (Color online) Computed FS sheets of URuAl existing in four conduction bands, drawn separately for each band in the reduced zone scheme with marked symmetry points in hexagonal BZ and some nesting vectors $\mathbf{q_1}$ and $\mathbf{q_2}\|c$ axis with lengths of 0.08 and 0.25 $(2\pi/c)$, respectively.

of positron-annihilation radiation (e.g., Ref. 31). Some possible nesting vectors $\mathbf{q}_1$ and $\mathbf{q}_2$ are marked in Fig. 3.

Based on spin and orbital-polarized calculations for LSDA and LSDA+OPC, respectively, two different FM states, i.e., with different values of total ordered magnetic moments, were found self-consistently and are tabulated in Table I.

It is visible that in the case of LSDA calculations the values of the antiparallel spin and orbital magnetic moments on an uranium atom almost compensate each other, yielding the total magnetic moment of −0.19 μ_B, so that the magnetic polarization nearly vanishes. This is not a case, however, when OPC is taken into account in calculations to the uranium 5*f* states, which leads to marked values of the ordered moments. However, our practice shows that OPC usually gives overestimation of the moments for 5*f* electrons. There is a small difference in total energy (~0.5 mHartree) between nonmagnetic LDA and FM LSDA states, the latter being the ground state, which may be the reason for difficulties in stabilizing the FM state, in addition having such a small value (~0.2 μ_B) of the uranium ordered moment. It is worth noticing that the total magnetic moment on an U atom in URuAl induced in the applied field of 5 T (at $T=50$ K when χ reaches its broad maximum) and measured by polarized neutrons[11] is even smaller (0.042 μ_B) than that obtained from our LSDA calculations (−0.19 μ_B). Both the LSDA

TABLE I. Values of ordered spin (μ_s), orbital (μ_l), and total (μ_{tot}) magnetic moments in μ_B per an atomic position in the unit cell.

	LSDA				LSDA+OPC			
Atomic position	μ_s	μ_l	μ_l/μ_s	μ_{tot}	μ_s	μ_l	μ_l/μ_s	μ_{tot}
U	0.64	−0.83	−1.30	−0.19	1.26	−2.74	−2.18	−1.48
Ru(1)	−0.06	−0.02	0.33	−0.08	−0.10	−0.11	1.1	−0.21
Ru(2)	−0.05	−0.00	0.00	−0.05	−0.08	−0.08	1.0	−0.16
Al	−0.01	−0.00	0.00	−0.01	−0.01	−0.01	1.0	−0.02

and LSDA+OPC results reproduce the experimental tendency that the total magnetic moment induced on the Ru(1) is higher than that on the Ru(2) position.

The computed (total and partial contributions) and experimental XPS valence-band spectra are presented in Fig. 4. The latter are shown after subtracting the experimental background using the Tougaard method.[32] It is apparent that the spectrum has a triple-peak structure. In the theoretical spectrum the first large peak crossing E_F comes mainly from the large contribution from the U $5f_{5/2}$ states (dominating to about 1 eV BE below E_F). In addition, this peak contains also very small contributions from the U $6d$ and the ruthenium $4d$ states, forming metallic bonding. The second peak, being almost of the same magnitude as the former one and occurring in the energy range about 1–5 eV below E_F, is slightly split at its top into two peaks, centered at BE of −2.0 and −2.58 eV.

This split peak is formed mainly by the contributions originating from the Ru(1) and Ru(2) $4d$ states, the latter ones being the biggest in this energy range, and also due to the pronounced contribution of the U $5f$ states (down to –4.2 eV). The U $6d$ states form a small and quite constant contribution ranging from E_F down to −6 eV. The third peak of a much smaller intensity than the two large former peaks described above is centered at –5.5 eV and formed mainly by the ruthenium $4d$ states. The contributions of the Al states, visible in Fig. 2, are completely diminished by the photoionization cross sections and cannot be detected by the XPS measurements. As seen, the theoretical XPS spectrum is in good agreement with the experimental one, especially as to the shape and positions of particular peaks. The lack of the O($2s$) line centered at about 6 eV BE indicates practically the lack of contamination by oxygen in the sample. Concluding, it is clear that these spectra show a highly delocalized character of the U $5f$ electrons and their quite wide contribution ranging at least down to energies of 4.2 eV.

The structure of the U $4f$ core lines is presented in Fig. 5. One can infer from it some essential information on the final states in the photoemission processes, which in this case is rather simple and well resolved. These lines have been decomposed according to the Doniach-Šunjić theory[33] (after subtracting the background by the Tougaard method[32]) into two highly asymmetric $4f_{5/2}$ (−388.6 eV) and $4f_{7/2}$ (−377.6 eV) main sublines, split by the spin-orbit interaction by 11 eV. It turns out that each main subline is accompanied only by one so-called 1 eV satellite, centered at −378.2 eV and −389.4 eV (sat. 1 in Fig. 5). A high asymmetry of the main U $4f$ sublines and the lack of so-called 7 eV satellite (at about −385 eV) are usually ascribed to strong U $5f$-$6d$ hybridization effects.[34] Moreover, the complete lack of the 3 eV satellite (at −380 eV) points to both no contamination of the sample by uranium oxides and no evidence for an additional final state of $5f^3$ [i.e., exactly at the position like that in UO_2 (Ref. 35)]. The lack of contamina-

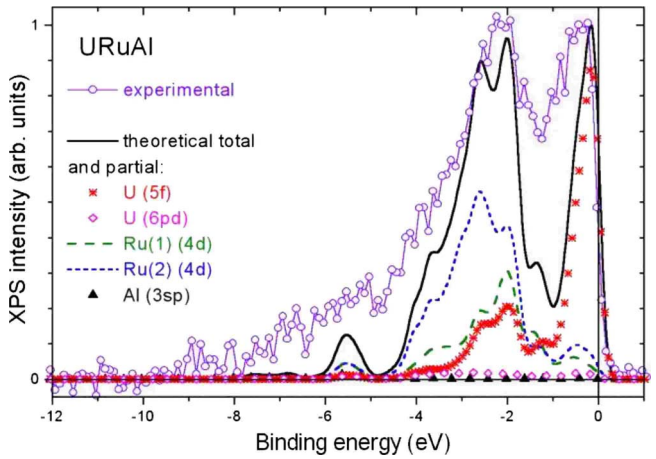

FIG. 4. (Color online) URuAl: the experimental total valence-band XPS spectrum (after subtracting background) compared to the calculated total spectrum and its partial contributions from the different electronic states of atoms.

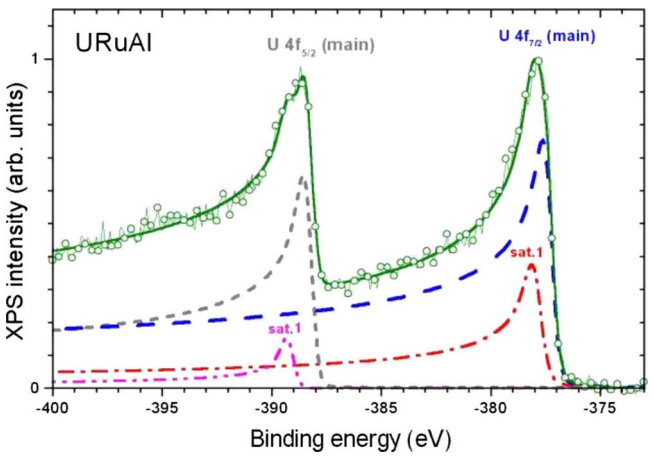

FIG. 5. (Color online) The experimental XPS of the U $4f$ core lines in URuAl. The lines are decomposed into the main sublines $4f_{5/2}$ and $4f_{7/2}$ and their single satellites (sat. 1).

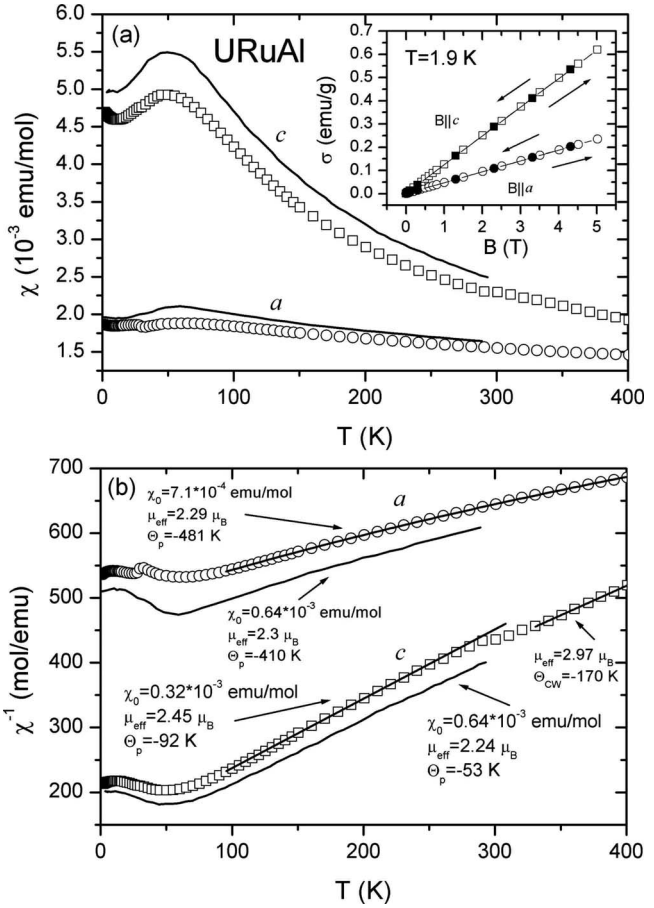

FIG. 6. (a) Molar susceptibility $\chi(T)$ measured along the a and c axes (open symbols) compared to previous results from Ref. 6 (lines). The insert shows magnetization in applied fields up to 5 T measured at $T=1.9$ K along the a and c axes with increasing and decreasing fields (open and closed symbols, respectively). (b) Inverse molar susceptibility, $\chi^{-1}(T)$ along a and c axes compared to the results from Ref. 6.

tion of the sample by oxides seems to be confirmed additionally by the lack of a visible anomaly in the valence-band XPS around 6 eV below E_F, despite a small trace of the peak O(1s) that is slightly seen in the overall spectrum of URuAl (not presented here).

B. Bulk magnetic and electron transport properties

Figure 6 presents results of susceptibility measurements on a single crystal of URuAl along the main crystallographic axes a and c taken at temperatures 1.9–400 K and $B=0.5$ T. The obtained results are compared to those previously published.[6] They were obtained in the temperature range 4.2–300 K also using a single crystal of URuAl. As seen, there are some differences in absolute values between these two measurements, but the character of the temperature dependences of the susceptibilities [Fig. 6(a)] or their reversals [Fig. 6(b)] is almost the same. The small differences can occur due to a possible grain misalignment and/or an existing deviation from stoichiometry and even probably because of using different calibration standards. For the $\chi_c^{-1}(T)$ curve we observed some inflection point at about 300 K and the effective moment we have calculated applying a simple CW law over only a narrow temperature range above this temperature. Hence, the magnetic parameters are different from those given in Ref. 6. However, when we use in calculations the modified CW law between 100 and 300 K the obtained parameters appear to be closer to each other as also those for the $\chi_a^{-1}(T)$ behavior (see the corresponding values in this figure). It is clear that, as it was reported previously,[6] there exists really strong uniaxial anisotropy in the paramagnetic behavior.

The difference $\Delta\Theta_p=(\Theta_p^c-\Theta_p^{ab})$ is, like the previous results, around a huge value of about 570 K. It is worthwhile noting that there is no difference in the temperature of the susceptibility maximum, $T_{\chi_{\max}}$, amounting in both cases about 50 K. In the inset of Fig. 6(a) we present the magnetization taken for URuAl at 1.9 K measured along both crystallographic directions in increasing and decreasing applied fields up to 5 T. It is clear that they present a linear behavior without a trace of hysteresis with very small moments reaching the values of 0.041 μ_B and 0.016 μ_B at $\mu_0 H=5$ T for the easy and hard magnetization axes, respectively. These results are in good agreement with the high magnetic-field measurements of the magnetization performed on a single-crystalline sample of URuAl up to 35 T.[6] The latter shows, however, an upturn deviation from the straight-line behavior measured along the c axis at fields as high as 20 T. It is rather reminiscent of some metamagnetic transition than forming a magnetically correlated state as was reported for URuGa.[23] No such deviation, however, was observed for the a axis up to 35 T. Hence, these two ternaries URuAl and URuGa, for which the high-field magnetizations were done[10] some time ago, are examples of having very stable ground states in comparison, e.g., to UCoAl, where a magnetic field as small as about 1 T is enough to cause the metamagneticlike transition.[1] This is not surprising because URhAl with almost the same number of ds electrons as has the former compound is already ferromagnetic with $T_C=35$ K.[36] Also even a very slight concentration of Fe or Ru doped to UCoAl, which leads to significant lowering the number of ds electrons, immediately causes the occurrence of FM. This aspect of the behavior will be discussed later.

In Fig. 7 the electrical resistivity, $\rho(T)$, is displayed, measured with the current **j** directed parallel to the a and c axis. As seen from this figure, both these characteristics are very similar to each other. At low temperatures the AT^2 law is followed up to about 30 K, as shown in the figure, where the corresponding parameters are also presented. For the spin-fluctuation case a pronounced T^2-like increase of $\rho(T)$ at low temperatures is predicted by the theory.[37]

The factor A is related to the corresponding spin-fluctuation temperatures by $A\sim(T_{\mathrm{SF}})^{-2}$. However, it is common for other spin fluctuators that the factor A is dependent on the current direction applied in a single crystal. Next, the resistivity of URuAl goes through a broad knee around $T=75$ K and then it exhibits a wide flat maximum around 100 K. Above this temperature $\rho(T)$ for both directions decreases slightly up to RT. As shown in Ref. 38, calculations of the temperature variation of $\rho_{\mathrm{SF}}(T)$ for actinide compounds such as UAl_2 have shown the decrease of the resistivity in the

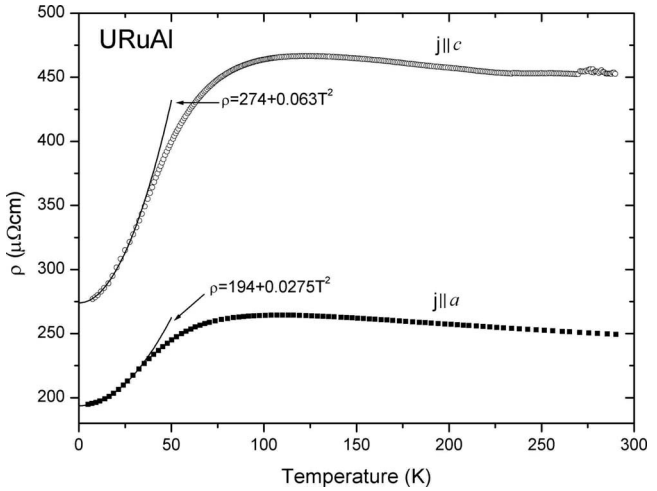

FIG. 7. Electrical resistivity, $\rho(T)$, of URuAl measured for the current applied parallel to the a and c axes. The solid lines show the AT^2 dependencies.

high-temperature region after a subtraction of the phonon contribution.

The absolute values of the resistivity are rather high due to the large values of the residual resistivities but all these values are in the highest limits of semimetals. This behavior is more reminiscent of that exhibited by spin fluctuator $PuAl_2$ (Refs. 39 and 40) than that of the S-type shaped runs found for the classical spin fluctuators of UAl_2 (Ref. 40) or UPt_3.[41]

The magnetoresistivity (MR), defined as $\Delta\rho/\rho_0=|\rho(B)-\rho(0)|/\rho(0)$, has been measured for a current direction parallel to the a and c axes with an applied magnetic fields up to 8 T being always directed perpendicular to the current. The obtained results are shown in Figs. 8(a) and 8(b), respectively. As seen, the absolute MR values for both directions are very small. Due to this fact accuracy of the MR measurements is rather poor. Moreover, they have at low temperatures a different sign; that along the a axis is mainly negative (except for a small field range at 4.2 K where this is positive), while that along the c axis measured at temperatures 4.2, 10, and 25 K is positive following the $a(T)B^2$ dependence. This tendency is changed at 50 K where MR becomes negative in all fields up to 8 T.

In the inset of Fig. 8(a) we present the temperature variation of MR (measured up to 70 K) for the current direction along the a axis only at a field of 8 T. One can see a very small positive maximum in $\Delta\rho/\rho_0(T)$ at 20 K which also appears for a curve determined from values taken at $\mu_0 H=8$ T of Fig. 8(a), but at this time all values are slightly negative. Although there is a distinct difference in the absolute values owing to small accuracy of measurements, the characters of these two curves are similar to each other. At first glance it appears that an explanation of the obtained MR data in terms of a spin-fluctuation (SF) model seems to be not convincing since one expects a distinct depressing of the SF contribution to the resistivity by an applied magnetic field predicted by theory.[42,43]

Usually two contributions to MR can be distinguished, i.e., the ordinary MR, being always positive, is due to the orbital motion of the electrons in a magnetic field, often called as a Lorentz type of contribution, and that arising from the scattering of the conduction electrons by the SFs, being always negative. The former decreases itself when T increases. So that at higher temperatures the negative MR might indicate spin fluctuations in both compounds, URuAl and URuGa.

Such small MR values as observed in URuAl and URuGa,[23] often having a positive sign at low temperatures and in low magnetic fields, have been found also in other SF

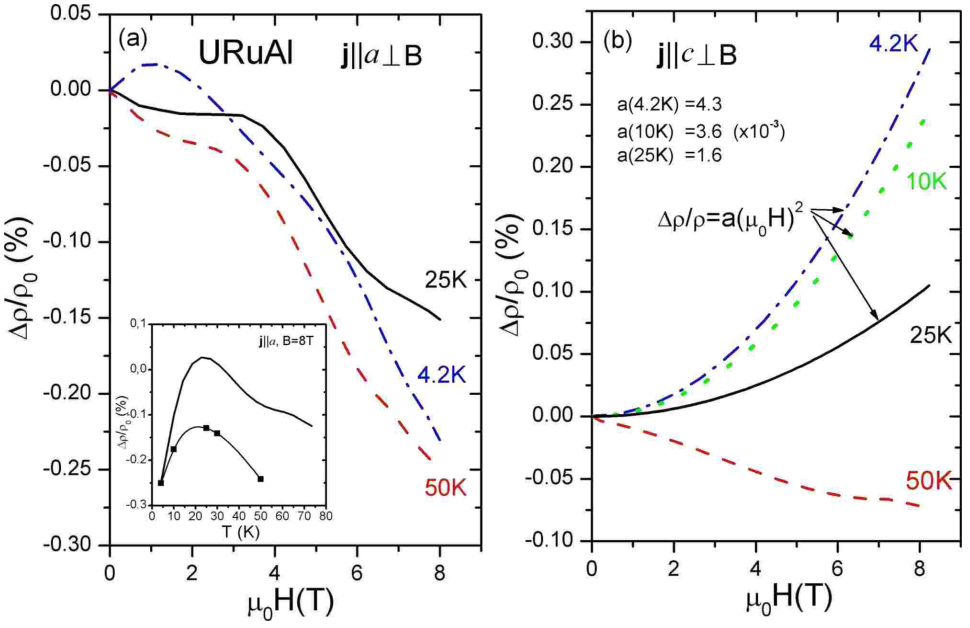

FIG. 8. (Color online) Isothermal transverse magnetoresistivity $\Delta\rho/\rho_0$ for the current direction **j** parallel to the a and c axes, parts (a) and (b), respectively, with applied magnetic fields up to 8 T. Inset of part (a) shows the temperature variation up to 70 K for **j** along the a axis at a field of 8 T. The squares indicate the MR values taken at 8 T from the isothermal MR curves.

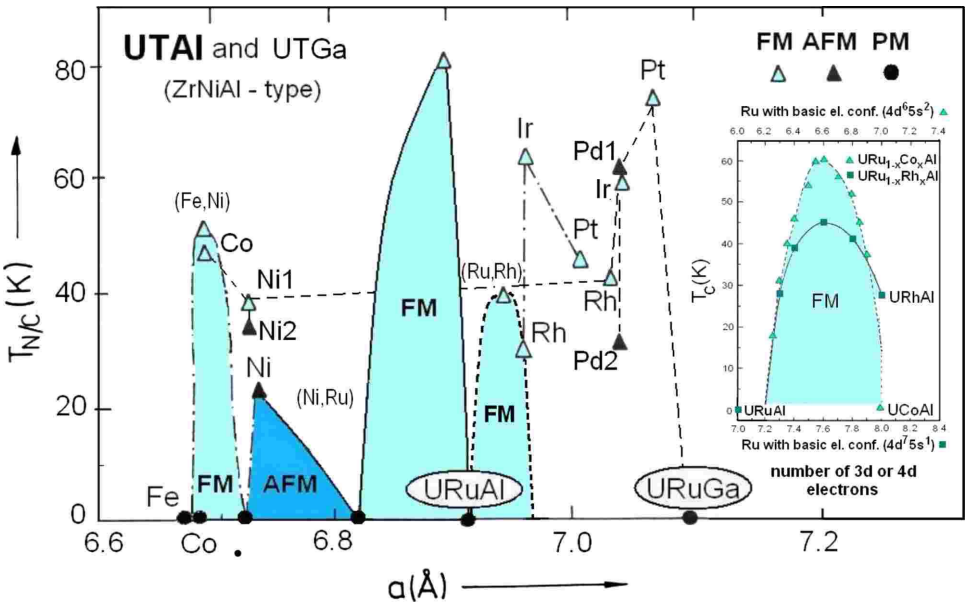

FIG. 9. (Color online) Magnetic phase diagram for the UTAl and UTGa systems (crystallizing in the ZrNiAl-type structure) showing dependence of the ordering temperatures $T_{N/C}$ on the lattice parameter a. For the former system the same is given for some solid solutions (see marked areas). The insert shows the basic electron configuration of Ru in the U(Ru,Co)Al (top scale) and U(Ru, Rh)Al (bottom scale) solid solutions assuming either $4d^6 5s^2$ [analogous to those for Fe ($3d^6 4s^2$)] or $4d^7 5s^1$, respectively. In both cases the difference to the Co-or Rh-based systems is equal to one electron d.

compounds as UAl_2,[44] UPt_3,[45] and TCo_2.[46] As pointed out in Ref. 47, for example, a suppression of spin fluctuations in UAl_2 could be possible only in applied fields between 15 and 20 T.

V. DISCUSSION

Any magnetic material is mainly characterized by the magnetic transition temperature $T_{C/N}$ and the type of magnetic order. For the ZrNiAl type crystal structure usually we have to do with a linear magnetic order with an easy magnetization c axis. Owing to a layered type of the above crystal structure and the predominant magnetic interaction within four U nearest neighbors of the uranium central atom (in the basal plane) at a distance $d_{U\text{-}U} \approx 0.52a$, huge anisotropy in such a material takes place even for the nonmagnetic URuAl and URuGa. In order to understand such a behavior of these compounds we have built up the magnetic phase diagram (MPD) shown in Fig. 9. This figure presents the ordered temperature $T_{C/N}$ mainly of the UTAl systems[48] and for some solid solutions such as U(Fe, Ni)Al,[16] U(Ni, Ru)Al,[49] and U(Ru,Rh)Al.[10] All these solutions exhibit continuous solubility over the entire concentration range. The former two alloys show in a well-established composition range FM but those for compositions around UNiAl AFM (see the shaded areas in Fig. 9). The U(Ru, Rh)Al alloys are completely ferromagnetic when containing more than 20 mol % of Rh. In addition, large black circles on this diagram denote compositions showing the quantum critical point (QPC). It is interesting that both URuAl and URuGa (the latter is also placed on this diagram) thus can be considered as those exhibiting such a point (nonmagnetic state) despite the fairly large difference in the U-U distances (about 0.013 nm) and hence some distant location on this MPD.

As seen, URuAl having a smaller lattice parameter (a=0.687 nm) than URuGa (0.712 nm) occurs between two areas of the FM behavior, formed from on one hand by the U(Ni,Ru)Al solid solutions above 15 mol % of Ru (Ref. 49) and for the U(Ru,Rh)Al ones above 20 mol % of Rh on the other hand.[10] Thus, based on such a behavior, one sees that the U-U distance needed to create QCP is not a decisive factor in forming an ordered or nonordered states in these systems. Moreover, in the inset of Fig. 9 we have plotted the critical temperatures T_C for both solid solutions U(Ru,Co)Al (Ref. 14) and U(Ru,Rh)Al (Ref. 10) against the number of $3d$ ($4d$) or $4d$ electrons. The latter was calculated in the simplest way using a nominal atomic configuration and by assuming a difference of one electron $3d$ ($4d$) between the Ru and Co or Rh atoms. It is clear that a maximum in T_C (for the data taken from Refs. 14 and 10, respectively) is reached for about 6.7 (or 7.6) of the $3d$ ($4d$) electrons per f.u. for both systems. It is worth noticing that despite the smallest d_{U-U} distances found in the case of solid solutions U(Fe-,Co)Al (Ref. 50) and U(Fe,Ni)Al,[16] the maximum in T_C also was found for nearly the same concentration of $3d$ electrons.[50] We do not know real d or other electron concentrations in a particular system but the difference between various systems forming, e.g., solid solutions certainly exists and thus this decides about the exhibited magnetic behavior, i.e., in raising magnetic ordering or its disappearing. Our band-structure calculations for both URuAl and URuGa (Ref. 23) give slightly more than seven $4d$ electrons per f.u. while the number of $5s$ electrons is much less than unity per f.u. To make detailed comparison one should perform such calculations for other ternary UTM compounds and their

common solid solutions, which extends beyond the frames of this paper. In conclusion, the considered here diagram also manifests the most important role of the number of $3d$ ($4d$) electrons in the QCP rising. In these systems, a concentration of d electrons can be treated as a control parameter of QCP reflected by changing their composition x. In any deeper analyses, of course, one should take into account not only the proper nd concentrations but also those of the s,p electrons in the system. Summarizing, one sees that a continuous change in the conduction electrons concentration in all systems mentioned above may help to understand the creation of the magnetically ordered state displaying a maximum in the $T_{C/N}(x)$ curve when mixing some two nonmagnetic UTM ternaries or as is the case of U(Ni,Ru)Al magnetically ordered and nonmagnetic ones.

A similar consideration made for URuGa, leads to the conclusion that this compound in contrast to URuAl is located with its a lattice parameter at the end of the whole UTGa family for which the ordering temperatures were also partly plotted on the MPD in Fig. 9. We are, however, not aware of such existing data for the solid solutions between URuGa and its nearest lying neighbor on this diagram, namely, UPtGa. Nevertheless, several publications have been devoted to the system U(Ni,Ru)Ga,[15] but closer to our analysis here does appear the U(Ru,Pd)Ga system,[51] where the difference in the number of $4d$ electrons, however, is equal to 2. With increasing Pd compositions as many as three different magnetic states are observed, the FM state is stable in a wide concentration range between 10 and 80 mol % of Pd, the ferrimagnetic ordering is found for about 80 mol % of Pd, and, finally, the AFM spin-arrangement of sine-modulated type exists for 90 and 100 mol % of Pd.

Such a difference in $3d$ ($4d$) concentration exists also in the solid solutions U(Ni,Fe)Al and U(Ni,Ru)Al. As seen from the MPD presented in Fig. 9, the difference in the d electron concentration in these systems changes from 2 to 0 and then one observes the conversion from AFM to FM and finally to PM, almost exactly like that in the U(Ru,Pd)Al system. Again the latter phenomenon strongly emphasizes the role of the number of conduction electrons and the extend of their hybridization with the U $5f$ electrons.

The band-structure calculations, presented so far for URuAl only in Refs. 20–22, contrary to that described above, do not include the SOC and the contributions to DOS (presented only in Fig. 4 in Ref. 21) coming from the U $5f$ states are much different from our results (see Fig. 2), yielding DOSs which are cut by the Fermi level in the minimum with the magnitude being almost two times smaller than our DOS, whereas the positions of ruthenium $4d$ states (displayed together) are quite similar to our results. Furthermore, our DOS and XPS spectra (Figs. 1, 2, 4, and 5) are very similar to the data obtained for isostructural paramagnet URuGa,[23] differing mainly in BE positions of the Al and Ga contributions, centered at 5.5 and 6.5 eV, respectively. However, their Fermi surfaces, existing for both compounds in four bands, are much more different from each other in both the shape and size of FS sheets,[52] but in both cases elements along the hexagonal c axis are disconnected and have geometry typical of nesting[30] that may mediate in magnetic interactions, connected with magnetic fluctuations. The analogous tendency of magnitude of the ordered magnetic moments is observed in both compounds[52] that can be responsible for magnetic instabilities leading to magnetic fluctuations.

Predominant metallic-type bonding in URuAl is created due to relatively strong hybridization effects of mainly the U $5f$ and $6d$ states as well as, in smaller degree, with the Ru(1) and Ru(2) $4d$ states and the Al $3spd$ states, located around E_F (see Fig. 2). Owing to these effects the U $5f$ states become highly delocalized forming dispersive bands in the same wide energy range as the U $6d$ states, but especially those being close to E_F. The numbers (per atom) of above mentioned states, i.e., the U $6d$ and Al $3pd$ states, are considerably increased while those of the U $5f$ states are much reduced. The most interesting finding is that, although the distances between the U atom and the nearest Ru(1) and R(2) atoms are almost the same, the contributions of the Ru $4d$ states, in the hybridization with the U $5f$ states, originating from nonequivalent positions of these atoms in the unit cell, are essentially different from each other in an energy range of 2.5–4.5 eV below E_F. Thus, in this energy range the contribution from the ruthenium $4d$ states coming from the Ru(2) atom is in the form of a much broader peak than that from Ru(1) [see Fig. 2(b)]. Also the total charge transfer from uranium to the different Ru positions is completely different in both the sign and magnitude. It points to strongly anisotropic hybridization effects of the ruthenium $4d$ states. The evidence of anisotropic hybridization of the U $5f$ and ruthenium $4d$ states has been observed for URuAl in a polarized-neutron experiment by Paixão *et al.*[11] This phenomenon is responsible for inducing (by magnetic field) the magnetic moment on ruthenium $4d$ electrons but markedly only at the Ru(1) atomic position, i.e., those lying in the uranium plane, and probably this is responsible for a giant magnetic anisotropy seen in bulk measurements of this compound. This tendency is well reproduced by our spin and orbital polarized calculations. It may also suggest that in both compounds URuAl and URuGa the character of chemical bonding within the U-Ru(1) plane can be different from that in the (Ga,Al)-Ru(2) plane, as has been suggested in Refs. 16 and 17. In the latter work, this effect was considered theoretically in the case of the isostructural UFeAl compound, in which the corresponding bondings in U-Fe(1) and Al-Fe(2) planes have occurred to exhibit predominantly metallic and covalent characters, respectively.

We achieved good agreement between our theoretical and experimental XPS valence-band spectra measured on a high-purity single crystal. It confirms a high delocalization of the U $5f$ states and their anisotropic hybridization with the ruthenium $4d$ states originating from different atomic ruthenium positions. In turn, the $4f$ core-level spectrum is in a high degree asymmetric, which additionally points to the existence of the strong U $5f$-$6d$ hybridization effects. Moreover, a unique feature as is the presence of the only one asymmetric 1 eV satellite, observed also in URuGa,[23] has to be somehow connected with the spin-fluctuation effects. The more so as the lack of the 3 and 7 eV satellites suggests that URuAl is like URuGa rather only a magnetic-fluctuating compound than also mixed-valence one.

VI. CONCLUSIONS

(1) We have tried to answer in this paper the question why both the URuAl and URuGa ternaries are nonmagnetic, though they have the different $d_{\text{U-U}}$ distances but in both cases they are slightly larger than the Hill limit. This leads to their different position on the presented here magnetic phase diagram with respect to the $d_{\text{U-U}}$ magnitudes as well as to their various U*TM* neighbors.

(2) It seems that the answer lies in the number of *d* electrons in these two systems. It thus appears that the band-structure calculations yield for the Ru atom in both these compounds almost the same number of 4*d* electrons/f.u. close to 7.

(3) Our calculations also show that for both ternary compounds discussed here the magnitudes of spin and orbital moments for an U atom are almost equal and owing to their opposite directions in the case of any ordered state formation they would cancel each other, which in consequence, would not lead to the magnetic behavior of the above compounds at low temperatures. However, such a situation is capable to bring about a spin-fluctuation effect. Thus for these two compounds it is probably accomplished just for seven 4*d* electrons/f.u.

(4) As for the case of URuGa, we have found also for URuAl only the 1 eV satellite in its 4*f* core spectrum, which probably may be attributed to the spin-fluctuation effect in these two ternaries. The lack in such a spectrum of the other 3 and 7 eV satellites should be underlined, often occurring in many other intermetallic uranium compounds.

ACKNOWLEDGMENTS

We gratefully acknowledge K. Wochowski for obtaining the single crystal of URuAl and J. Stępień-Damm for making its orientation, as well as R. Gorzelniak and D. Badurski for their technical assistance. We are also grateful to B. Coqblin for a fruitful discussion.

[1] V. Sechovský, L. Havela, F. R. De Boer, J. J. M. Franse, P. A. Veenhuizen, J. Sebek, J. Stehno, and A. V. Andreev, Physica B & C **142**, 283 (1986).
[2] K. Prokes, F. Bourdarot, P. Burlet, P. Javorsky, M. Olsovec, V. Sechovsky, E. Bruck, F. R. de Boer, and A. A. Menovsky, Phys. Rev. B **58**, 2692 (1998).
[3] Q. G. Sheng and B. R. Cooper, J. Magn. Magn. Mater. **164**, 335 (1996).
[4] V. Sechovský, L. Havela, F. R. de Boer, P. A. Veenhuizen, and E. Brück, J. Phys. (Paris), Colloq. **49**, C-8 497 (1988).
[5] P. A. Veenhuizen, J. C. P. Klaasse, F. R. de Boer, V. Sechovský, and L. Havela, J. Appl. Phys. **63**, 3064 (1988).
[6] P. A. Veenhuizen, F. R. de Boer, A. A. Menovsky, V. Sechovsky, and L. Havela, J. Phys. **49**, C-8 485 (1988).
[7] V. Sechovsky, L. Havela, H. Nakotte, F. R. de Boer, and E. Bruck, J. Alloys Compd. **207-208**, 221 (1994).
[8] V. Sechovsky, L. Havela, F. R. de Boer, and E. de Brück, J. Alloys Compd. **181**, 179 (1992).
[9] F. R. de Boer, E. de Brück, A. A. Menovsky, P. A. Veenhuizen, V. Sechovsky, L. Havela, and K. H. J. Bushow, Physica B **155**, 221 (1989).
[10] V. Sechovsky, L. Havela, F. R. De Boer, P. A. Veenhuizen, K. Sugiyama, T. Kuroda, E. Sugiura, M. Ono, M. Date, and A. Yamagishi, Physica B **177**, 164 (1992).
[11] J. A. Paixão, G. H. Lander, A. Delapalme, H. Nakotte, F. R. Boer, and E. Brück, Europhys. Lett. **24**, 607 (1993).
[12] A. V. Andreev, V. Sechovsky, L. Havela, J. Sebek, M. I. Bartashevich, T. Goto, K. Kamishima, D. A. Andreev, V. S. Gaviko, R. V. Dremov, and I. K. Kozlovskaya, Czech. J. Phys. **46**, S6 (1996).
[13] A. V. Andreev, R. V. Dremov, M. I. Bartashevich, T. Goto, L. Havela, and V. Sechovsky, Physica B **230-232**, 68 (1997).
[14] A. V. Andreev, L. Havela, V. Sechovsky, M. I. Bartashevich, J. Sebek, R. V. Dremov, and I. K. Kozlovskaya, Philos. Mag. B **75**, 827 (1997).
[15] A. V. Andreev, V. Sechovsky, L. Havela, M. I. Bartashevich, T. Goto, R. V. Dremov, and I. K. Kozlovskaya, Physica B **237-238**, 224 (1997).
[16] R. Troć, V. H. Tran, F. G. Vagizov, and H. Drulis, Phys. Rev. B **51**, 3003 (1995); V. H. Tran, R. Troć, and H. Nöel, J. Alloys Compd. **262-263**, 471 (1997).
[17] I. M. Reznik, F. G. Vagizov, and R. Troć, Phys. Rev. B **51**, 3013 (1995).
[18] A. V. Andreev, L. Havela, V. Sechovsky, H. Aruga Katori, and T. Goto, J. Alloys Compd. **235**, 72 (1996).
[19] V. Sechovský, L. Havela, L. Neužil, A. V. Andreev, G. Hilscher, and C. Schmitzer, J. Less-Common Met. **121**, 169 (1986).
[20] T. Gasche, S. Auluck, M. S. S. Brooks, and B. Johansson, J. Magn. Magn. Mater. **104-107**, 37 (1992).
[21] T. Gasche, M. S. S. Brooks, and B. Johansson, J. Phys.: Condens. Matter **7**, 9499 (1995).
[22] T. Gasche, M. S. S. Brooks, and B. Johansson, J. Phys.: Condens. Matter **7**, 9511 (1995).
[23] M. Samsel-Czekała, E. Talik, R. Troć, and J. Stępień-Damm, Phys. Rev. B **77**, 155113 (2008).
[24] FPLO-5.00–18, and 5.10–20 [improved version of the original FPLO code by K. Koepernik and H. Eschrig, Phys. Rev. B **59**, 1743 (1999)]; http://www.FPLO.de.
[25] E. Talik, M.-E. Lucas, W. Suski, and R. Troć, J. Alloys Compd. **350**, 72 (2003).
[26] J. P. Perdew and Y. Wang, Phys. Rev. B **45**, 13244 (1992).
[27] OPC implementation in FPLO5.10–20 according to O. Eriksson, M. S. S. Brooks, and B. Johansson, Phys. Rev. B **41**, 7311 (1990); Carsten Neise, "Orbital Polarization Corrections in Relativistic Density Functional Theory" Ph.D. thesis, Technische Universität, 2007; http://www.ifw-dresden.de/institutes/itf/diploma-and-phd-theses-at-the-itf.
[28] J. A. Paixão, A. Delapalme, W. Paulus, and E. Brück, Z. Kristallogr. **209**, 594 (1994).
[29] P. Marksteiner, P. Weinberger, R. C. Albers, A. M. Boring, and G. Schadler, Phys. Rev. B **34**, 6730 (1986).
[30] J. J. Yeh and I. Lindau, At. Data Nucl. Data Tables **32**, 1 (1985).

[31] S. B. Dugdale, H. M. Fretwell, M. A. Alam, G. Kontrym-Sznajd, R. N. West, and S. Badrzadeh, Phys. Rev. Lett. **79**, 941 (1997); M. Biasini, G. Kontrym-Sznajd, M. A. Monge, M. Gemmi, A. Czopnik, and A. Jura, *ibid.* **86**, 4616 (2001); D. Hughes, M. Däne, A. Ernst, W. Hergert, M. Lüders, J. Poulter, J. B. Staunton, A. Svane, Z. Szotek, and W. M. Temmerman, Nature (London) **446**, 650 (2007).

[32] S. Tougaard, J. Electron Spectrosc. Relat. Phenom. **52**, 243 (1990).

[33] S. Doniach and M. Šunjić, J. Phys. C **3**, 285 (1970).

[34] W.-D. Schneider and C. Laubschat, Phys. Rev. Lett. **46**, 1023 (1981); T. Gouder, L. Havela, M. Diviš, J. Rebizant, P. M. Oppeneer, and M. Richter, J. Alloys Compd. **314**, 7 (2001).

[35] H. Grohs, H. Höchst, P. Steiner, S. Hüfner, and K. H. J. Buschow, Solid State Commun. **33**, 573 (1980).

[36] A. V. Andreev and M. I. Bartashevich, Fiz. Met. Metalloved. **62**, 266 (1986).

[37] A. L. Schindler and M. J. Rice, Phys. Rev. **164**, 759 (1967).

[38] B. Coqblin, J. R. Iglesias-Sicardi, and R. Jullien, Contemp. Phys. **19**, 327 (1978).

[39] R. Jullien, M. T. Beal-Monod, and B. Coqblin, Phys. Rev. Lett. **30**, 1057 (1973).

[40] A. M. Boring, R. C. Albers, G. R. Stewart, and D. D. Koelling, Phys. Rev. B **31**, 3251 (1985).

[41] A. de Visser, J. J. M. Franse, and A. Menovsky, J. Magn. Magn. Mater. **43**, 43 (1984).

[42] K. Ueda, Solid State Commun. **19**, 965 (1976).

[43] P. Hertel, J. Appel, and D. Fay, Phys. Rev. B **22**, 534 (1980).

[44] J. M. van Ruitenbeek, A. P. J. van Deursen, H. W. Myron, A. J. Arko, and J. L. Smith, Phys. Rev. B **34**, 8507 (1986).

[45] A. de Visser, R. Gersdorf, J. J. M. Franse, and A. Menovsky, J. Magn. Magn. Mater. **54-57**, 383 (1986).

[46] A. T. Burkov, T. Nakama, M. Hedo, H. Niki, and K. Yagasaki, J. Magn. Magn. Mater. **226-230**, 677 (2001); E. Gratz, Physica B **237-238**, 470 (1997); T. Nakama, K. Shintani, K. Yagasaki, A. T. Burkov, and Y. Uwatoko, Phys. Rev. B **60**, 511 (1999).

[47] J. J. M. Franse, P. H. Frings, F. R. de Boer, A. Menovsky, C. J. Beers, A. P. J. van Deursen, H. W. Myron, and A. J. Arko, Phys. Rev. Lett. **48**, 1749 (1982).

[48] R. Troć, in *16émes Journées des Actinides, April 28–30, Eibsee/Germany*, 1986, Abstract Booklet, p. 39.

[49] A. V. Andreev, V. Sechovský, L. Havela, M. I. Bartashevich, T. Goto, R. V. Dremov, and T. K. Kozlovskaya, Physica B **237-238**, 224 (1997).

[50] V. H. Tran, R. Troć, A. J. Zaleski, F. G. Vagizov, and H. Drulis, Phys. Rev. B **54**, 15907 (1996).

[51] V. H. Tran, R. Troć, P. de V. du Plessis, G. André, and F. Bourée, Phys. Rev. B **56**, 11065 (1997).

[52] M. Samsel-Czekała (unpublished).